Resource Allocation for Networked Telemetry System of Mega LEO Satellite Constellations

Guanming Zeng, *Graduate Student Member, IEEE*, Yafeng Zhan, Haoran Xie, *Graduate Student Member, IEEE*, and Chunxiao Jiang, *Senior Member, IEEE*

***Abstract*— In the upcoming 6G communication era, the satellite Internet based on mega constellations will become an indispensable extension of the terrestrial communication network. However, it is difficult for the traditional ground-based and geostationary earth orbit (GEO)-based telemetry systems to satisfy the requirements on monitoring the mega constellation. This paper designs the networked telemetry system, where data is transmitted through the inter-satellite-links (ISL) of the low earth orbit (LEO) and medium earth orbit (MEO) satellites. Furthermore, the resource allocation problem for the networked telemetry system is decomposed using the block coordinate descent method into the access scheduling and the subchannel-power coordinate allocation subproblems, which are iteratively solved to optimize the resource allocation scheme. Finally, the simulation results shows that the proposed resource allocation algorithm effectively increases the transmitted data amount of the system and approximates the upper bound performance.**

***Index Terms*— Satellite constellation, network, telemetry, resource allocation.**

I. Introduction

A. Motivations

THE satellite Internet is a critical component of the future 6G communications [1], [2], [3]. In recent years, in order to provide high-speed and low-latency broadband Internet services, numerous mega constellation plans have been proposed. SpaceX planned to build the Starlink constellation composed of about 42000 LEO satellites and to provide communication services with 50 Mbps $\sim$ 150 Mbps data rate and 20 ms $\sim$ 40 ms delay [4]. Oneweb planned to build the Kuiper constellation composed of 1980 LEO satellites and to provide communication services with up to 595 Mbps data rate and 32ms delay [5]. Astra Space submitted an application to the Federal Communications Commission (FCC) on November 4, 2021 to deploy a constellation composed of more than 13,600 satellites to provide broadband services. China Satellite Network Group, established on April 28, 2021, integrated domestic mega constellation plans and resources including Hongyun and Hongyan, and aimed at building a Chinese version of Starlink.

In order to monitor the operation status of the mega constellation, the construction of the telemetry system is indispensable [6]. For the traditional ground-based telemetry system, data is directly transmitted from the LEO satellite to the ground station [7], which is commonly used and provides basic telemetry service. However, the visible arc between the ground station and the LEO satellite is limited in each orbital period, rendering full-time telemetry impossible. Although deploying ground stations all around the world may relieve the challenge of limited visible arc, this scheme requires huge expenses for system deployment and thus is not feasible for all countries. For the traditional GEO-based telemetry system, data is indirectly transmitted from the LEO satellites to the ground station via the relay of GEO satellites. However, long-distance relay links among the GEO satellite, the LEO satellite and the ground station would introduce severe signal attenuation and high propagation delay.

The above defects make the traditional ground-based and GEO-based telemetry systems inappropriate for mega constellations. Therefore, ISLs of MEO and LEO satellites are utilized to construct the networked telemetry system [8], where the telemetry data can be transmitted from the LEO satellites to the ground station via the ISLs among LEO and MEO satellites. Compared with the traditional ground-based telemetry system, the networked telemetry system realizes full-time telemetry utilizing ISLs. GEO satellites locate at the altitude of 36,000 km and MEO satellites locate at the altitude from 5,000 to 20,000 km. Since the propagation delay is linearly correlated with the link distance, and the signal attenuation is quadratically correlated with the link distance, compared with the traditional GEO-based telemetry system, the networked telemetry system significantly reduces the signal attenuation and propagation delay [8]. Therefore, the networked telemetry system is promising for the upcoming era of mega constellations.

Based on the architecture of the networked telemetry system, this paper formulates the coordinate optimization of the

Manuscript received 12 December 2021; revised 10 June 2022 and 15 August 2022; accepted 11 October 2022. Date of publication 14 October 2022; date of current version 19 December 2022. This work was supported by the National Natural Science Foundation of China under Grant 61971261/62131012 and Technology Project of the State Grid Corporation of China under Grant 5400-202255158A-1-1-ZN. The associate editor coordinating the review of this article and approving it for publication was S. Chatzinotas. *(Corresponding author: Yafeng Zhan.)*

Guanming Zeng and Haoran Xie are with the Department of Electronic Engineering and the Beijing National Research Center for Information Science and Technology (BNRist), Tsinghua University, Beijing 100084, China (e-mail: zgm18@mails.tsinghua.edu.cn; xiehr20@mails.tsinghua.edu.cn).

Yafeng Zhan and Chunxiao Jiang are with the Beijing National Research Center for Information Science and Technology (BNRist), Tsinghua University, Beijing 100084, China (e-mail: zhanyf@tsinghua.edu.cn; jchx@tsinghua.edu.cn).

Color versions of one or more figures in this article are available at https://doi.org/10.1109/TCOMM.2022.3214895.

Digital Object Identifier 10.1109/TCOMM.2022.3214895

access scheduling, the subchannel and power allocation as a mixed integer nonlinear programming problem, so as to maximize the transmitted data amount of the system. Moreover, the optimization problem is decomposed into the access scheduling problem and the subchannel-power coordinate allocation problem, which are iteratively solved to derive the resource allocation scheme. Furthermore, this paper constructs the upper bound problem and derives its globally optimal solution, whose performance serves as the upper bound of the original optimization problem. Finally, the simulation results verify that the proposed resource allocation algorithm effectively improves the transmitted data amount and approximates the upper bound performance.

B. Related Works

The networked telemetry system is a novel system for mega constellations, the basic concept of which is proposed in [8]. As far as we know, there is no existing research on resource allocation for networked telemetry system. Nevertheless, resource allocation of related systems are investigated in this section, which include the ground-based telemetry system, the GEO-based telemetry system, the terrestrial cellular communication network and the hybrid satellite-terrestrial communication network.

1) Resource Allocation of the Ground-Based Telemetry System: Dinc et al. [9] studied the ground station deployment scheme that provides an average backhaul capacity of 1.2 Gbps for aircraft and the multi-user beamforming algorithm for dual-polarized hybrid direct air to ground communication (DA2GC) antenna arrays. Vondra et al. [10] evaluated the DA2GC link capacity based on 4G technologies, and adopted 5G technologies such as Multi-User Multiple Input Multiple Output and coordinated beam steering to improve the DA2GC link capacity. Vondra et al. [11] proposed a joint resource scheduling scheme for aircraft beam selection and spectrum allocation in DA2GC, so that as few aircrafts as possible share the same beam, and thus each aircraft occupies as much bandwidth as possible. However, the ground-based telemetry system considers the direct air to ground communication, while the networked telemetry system mainly focuses on the MEO-LEO inter-satellite communications. The system architectures and working mechanisms are totally different, which means the resource allocation method in the ground-based telemetry system is not suitable for the networked telemetry system.

2) Resource Allocation of the GEO-Based Telemetry System: Zhu et al. [12] formulated a tandem queuing model to describe the data arrival of LEO satellites, the data forwarding of GEO satellites and the data downloading of ground stations. Wang et al. [13] proposed a two-stage heuristic algorithm based on hierarchical scheduling strategy to optimize the task scheduling of satellite networks. Wang et al. [14] constructed a resource scheduling mechanism based on repeated game to coordinate the data relay requests of different LEO satellites. Du et al. [15] proposed a multiple access and bandwidth allocation strategy to make full use of the relay via the GEO satellite. However, the GEO-based telemetry system mainly considers the scenario in which multiple satellites are served by one GEO satellite, while the networked telemetry system mainly focuses on the scenario in which multiple LEO satellites are served by multiple MEO satellites. Due to the lack of consideration on the coordinated resource allocation among multiple satellites, the resource allocation method in the GEO-based telemetry system can not be directly applied to the networked telemetry system.

3) Resource Allocation of the Terrestrial Cellular Communication Network: Fooladivanda et al. [16] studied the interplay of user association and resource allocation in heterogeneous cellular network consisting of macro base stations and pico base stations. Zhong et al. [17] maximized the sum-rate of the uplink MIMO cellular networks with device-to-device communications. Lohani et al. [18] focused on the cellular network where users perform uplink transmission utilizing the energy harvested from RF transmission of base stations and relay nodes. Specifically, the joint optimal time and power allocation problem was solved. Yu et al. [19] studied the integrated cellular and Wi-Fi network and elaborated the energy-aware design of the network selection, subchannel, and power allocation. In order to facilitate the relay deployment in remote areas, Jangsher et al. [20] optimized the resource block allocation and power control in a cellular network with energy-harvesting relays. In the terrestrial cellular communication network, the base stations and users have low motional dynamics and infrequent handovers. In contrast, for the networked telemetry system, the satellites have high motional dynamics and frequent handovers. Therefore, the resource allocation scenario considered in this paper is more complex, which requires further consideration on reducing the overhead on system handovers.

4) Resource Allocation of the Hybrid Satellite-Terrestrial Communication Network: Considering the high dynamics and frequent handovers of LEO satellites, Zhao et al. [21] proposed an energy-efficient deep reinforcement learning based channel allocation scheme for satellite Internet of Things. Ivanov et al. [22] studied the structure of hybrid multi-beamforming on LEO satellite and proposed a low-complexity spatial resource allocation method to reduce handovers. Destounis et al. [23] optimized the power allocation among multiple satellite beams to reduce the number of users without the required quality of service. Tang et al. [24] studied the resource allocation scenario in which LEO satellites share a GEO satellite's spectrum with beam-hopping, so as to maximize the transmission capacity for terrestrial users. Han et al. [25] introduced the rental service into LEO satellite communication network, which improves the utilization of unused resources to serve terrestrial users. However, the above studies do not consider the characteristics of telemetry data. Specifically, the generation rate of telemetry data is stable and limited, which means excessive resource allocated to the minority of satellites will decrease the resource utilization efficiency.

C. Contributions and Organizations

The main contributions of this paper are as follows:

(1) This paper jointly optimizes the access scheduling, channel and power allocation of the networked telemetry system.

Specifically, the access scheduling, channel and power allocation of the networked telemetry system can be modeled as the mixed integer nonlinear programming, which is a non-convex NP-hard problem. In order to solve this problem, the block coordinate descent method is first adopted to decompose the original problem into the access scheduling subproblem and the channel-power coordinate allocation subproblem. After that, the successive convex optimization technique and the time relaxation technique are adopted to solve the access scheduling subproblem, and a theoretically optimal algorithm are designed to solve the channel-power coordinate allocation subproblem.

(2) This paper analyzes the performance upper bound of the resource allocation problem in the networked telemetry system. By transforming the original resource allocation problem and relaxing the constraints, the feasible region is expanded and the upper bound problem is obtained. Through variable dimensionality reduction, the upper bound problem can be simplified to a problem only related to the channel matrix. Furthermore, the globally optimal solution of the upper bound problem is obtained progressively, and the upper bound performance of the original resource allocation problem is obtained.

(3) This paper verifies the performance of the proposed resource allocation algorithm by numerical simulation. Specifically, the convergence of the algorithm is first verified by iterative simulation, and the performance of the algorithm is then verified under different system parameters including the bandwidth of each beam of MEO satellites, the half beam width of MEO satellites, the maximum total transmission power of LEO satellites and the generation rate of telemetry data of LEO satellites. The simulation results show that the proposed resource allocation algorithm effectively improves the transmitted data amount of the system, and approximates the upper bound performance.

The rest of this paper is organized as follows: Section II introduces the architecture, mechanism and data transmission model of the networked telemetry system. Section III formulates the optimization problem that maximizes the transmitted data amount of the system. In Section IV, the optimization problem is decomposed into the access scheduling problem and the subchannel-power coordinate allocation problem, which are solved iteratively to derive the resource allocation scheme. In Section V, the upper bound problem is formulated and its globally optimal solution is derived, whose performance serves as the upper bound of the original resource allocation problem. In Section VI, the numerical simulations are carried out to verify the resource allocation performance. Section VII summarizes the paper and gives the conclusion.

II. System Model

A. System Architecture and Mechanism

Fig. 1 illustrates the networked telemetry system, which consists of the mission center, the ground station, the MEO satellites and the LEO satellites. LEO-LEO ISLs exist between two adjacent LEO satellites on the same orbital plane, MEO-MEO ISLs exist between two adjacent MEO satellites, and SGLs exist between the ground station and the visible MEO satellite.

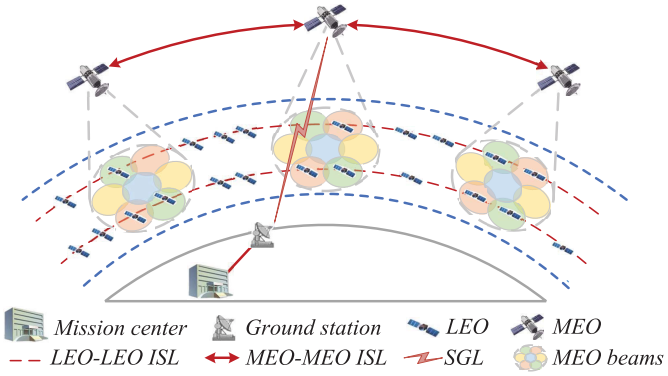

Fig. 1. The networked telemetry system.

As a system for monitoring the operation status of LEO satellites, the networked telemetry system is supposed to be robust even in case of malfunction of the LEO satellite attitude control. Considering the antenna may fail to be oriented to the MEO satellite that is scheduled for data reception, omni-directional antenna is equipped by LEO satellites to guarantee the communication regardless of any abnormal attitude. As for MEO satellites, directional antennas are equipped and the beams are well-designed to avoid signal interference. Since beams of different MEO satellites do not overlap with each other, the signals in beams of different MEO satellites are spatially isolated. For adjacent beams of the same MEO satellite, although overlap exists, different polarization modes or frequency bands are adopted to isolate signals in orthogonal channels without interference. For non-adjacent beams of the same MEO satellite, although the same polarization mode and frequency band may be utilized, there exists no coverage overlap and the signal power is limited. Therefore, interference between non-adjacent beams could be almost neglected. Within each MEO beam, frequency division multiplexing is adopted, and signals from different LEO satellites occupy different frequency orthogonal channels to avoid interference.

For the LEO satellite beyond the beam coverage, the data is transmitted to the LEO satellite within the beam coverage through the LEO ISLs on the same orbital plane. For the LEO satellite within the beam coverage, the data is first transmitted to the MEO satellite through the LEO-MEO ISLs, then transmitted to the ground station and mission center through the MEO ISLs and SGLs. Since the satellite orbits are fixed, the system topology throughout any orbital period can be predicted by orbit propagation. According to the obtained system topology, the mission center is able to calculate the resource allocation scheme throughout the orbital period. Subsequently, the resource allocation scheme is uploaded and stored in each satellite via the satellite telecommand system. Finally, data is transmitted by each LEO satellite and received by each MEO satellite according to the pre-loaded scheme. Specifically for each LEO satellite, the resource allocation scheme defines the accessed MEO beam, the occupied channels and the transmission power in each time slot.

There are two situations in which a handover occurs. One is that when a LEO satellite is located within the coverage

overlap of two adjacent beams of the same MEO satellite, the LEO satellite may access different beams on two consecutive time slots. The other is that if a LEO satellite does not access any MEO beam on the previous time slot, and access a MEO beam on the current time slot, then a handover occurs. Since particular polarization mode and frequency band are adopted for each MEO beam, during a handover, the LEO satellite changes the polarization mode and frequency band of the transmission signal to fit the MEO beam that is switched to.

B. The Telemetry Data Transmission Model

The LEO-LEO ISLs, MEO-MEO ISLs and MEO-ground SGLs of the networked telemetry system are fixed point-to-point links, so the data transmission model is intuitive and there are no complicated resource allocation problems. However, there are complex access scheduling, channel and power allocation problems for the LEO-MEO ISLs, whose transmission model is the focus of this paper and will be elaborated in this section. Assuming that there are I LEO satellites, each of which is equipped with an omni-directional antenna, and that there are J MEO satellites, each of which is equipped with K fixed directional beams. The total bandwidth of each beam is B and is divided into L subchannels. Here we define $\mathcal{I} = \{1, 2, \ldots, I\}, \mathcal{J} = \{1, 2, \ldots, J\}, \mathcal{K} = \{1, 2, \ldots, K\}$. The access matrix is defined as $\mathbf{A}_{I\times J\times K}$ with element $a_{i,j,k} \in \{0, 1\}$. If the *i*-th LEO satellite is connected to the *k*-th beam of the *j*-th MEO satellite, $a_{i,j,k} = 1$; otherwise, $a_{i,j,k} = 0$. The channel matrix is defined as $\mathbf{B}_I$ with element $b_i \in \mathbb{Z}^+$ representing the number of subchannels allocated to the *i*-th LEO satellite. The power matrix is defined as $\mathbf{P}_I$ with element p_i representing the transmission power of the *i*-th LEO satellite.

The signal propagates in a single path of the vacuum environment along the LEO-MEO ISLs, which can be modeled as the Gaussian channel. The channel power gain from the *i*-th LEO satellite to the *k*-th beam of the *j*-th MEO satellite mainly depends on the free space propagation loss and the antenna gain of the transceiver:

$$|h_{i,j,k}|^2 = G^t G^r_{i,j,k} \cdot \left(\frac{c}{4\pi f d_{i,j}}\right)^2, \tag{1}$$

where G^t is the omni-directional antenna transmission gain of the LEO satellite, $G^r_{i,j,k}$ is the directional antenna reception gain from the i-th LEO satellite to the k-th beam of the j-th MEO satellite, f is the carrier frequency, $d_{i,j}$ is the distance between the i-th LEO satellite and the j-th MEO satellite, and c is the light speed. Specifically, if the i-th LEO satellite is within the coverage of the k-th beam of the j-th MEO satellite, $G^r_{i,j,k} = G^r$; otherwise, $G^r_{i,j,k} = 0$. The signal-to-noise ratio (SNR) from the i-th LEO satellite to the k-th beam of the j-th MEO satellite is

$$\gamma_{i,j,k} = \frac{|h_{i,j,k}|^2 \cdot a_{i,j,k} \cdot p_i}{\sigma^2}, \tag{2}$$

where σ^2 is the noise power spectral density. According to the Shannon formula, the data rate is

$$R_{i,j,k} = \frac{B}{L} \cdot a_{i,j,k} \cdot b_i \cdot \log_2\left(1 + \frac{|h_{i,j,k}|^2 \cdot p_i}{\sigma^2}\right). \tag{3}$$

Different from the terrestrial network, due to the long spatial distance of ISLs, once access handover occurs, propagation delay $\frac{d_{i,j}}{c}$ and link reestablishment delay t_0 are introduced, and thus the total introduced delay can be deduced as $\left(\frac{d_{i,j}}{c} + t_0\right) \cdot \left|a_{i,j,k} - a^{pre}_{i,j,k}\right|$, where $a^{pre}_{i,j,k}$ represents the access of the previous time slot. Specifically, if $a_{i,j,k} = 1$ and $a^{pre}_{i,j,k} = 0$, then the total introduced delay is $\frac{d_{i,j}}{c} + t_0$; if $a_{i,j,k} = 1$ and $a^{pre}_{i,j,k} = 1$, or $a_{i,j,k} = 0$, then the total introduced delay is 0. Dividing the orbital period into multiple time slots with length T, the transmitted data amount from the i-th LEO satellite to the k-th beam of the j-th MEO satellite in the current time slot is

$$W_{i,j,k} = \frac{B}{L}\left(T - \left(\frac{d_{i,j}}{c} + t_0\right) \cdot \left(a_{i,j,k} - a^{pre}_{i,j,k}\right)\right) \cdot a_{i,j,k} \cdot b_i \cdot \log_2\left(1 + \frac{|h_{i,j,k}|^2 \cdot p_i}{\sigma^2}\right). \tag{4}$$

It is worth noting that, since $a_{i,j,k}, a^{pre}_{i,j,k} \in \{0, 1\}$, $\left|a_{i,j,k} - a^{pre}_{i,j,k}\right| \cdot a_{i,j,k}$ can be equivalently transferred into $\left(a_{i,j,k} - a^{pre}_{i,j,k}\right) \cdot a_{i,j,k}$. And the transmitted data amount of the system W and that of the i-th LEO satellite W_i are deduced as:

$$W = \sum_{i=1}^{I} W_i = \sum_{i=1}^{I}\sum_{j=1}^{J}\sum_{k=1}^{K} W_{i,j,k}. \tag{5}$$

III. Problem Formulation

Since the transmitted data amount W in each time slot should be maximized by adjusting the access matrix $\mathbf{A}$, the channel matrix $\mathbf{B}$ and the power matrix $\mathbf{P}$, the objective function can be formulated as (6a). Then we discuss the constraints of the networked telemetry system. As shown in (6b), the transmission power of each LEO satellite should not exceed the maximum power limitation $p_{\max}$. As shown in (6c), each LEO satellite can only access one beam of one MEO satellite. As shown in (6d), up to L subchannels can be allocated to the LEO satellites for each beam. As shown in (6e), the transmitted data amount of the i-th LEO satellite should not exceed its cached data amount D_i. As shown in (6f), in order to prevent inter-beam interference of the same polarization and frequency band, the power on any single subchannel shall not exceed $I_{\max}$. As shown in (6g), element values of the access, channel and power matrices should be consistent with their definitions. Based on the above analysis, the optimization problem is formulated as:

$$\max_{\mathbf{A},\mathbf{B},\mathbf{P}} \; W(\mathbf{A}, \mathbf{B}, \mathbf{P}) \tag{6a}$$

$$s.t.\; b_i \cdot p_i \le p_{\max}, \quad \forall i, \tag{6b}$$

$$\sum_{j=1}^{J}\sum_{k=1}^{K} a_{i,j,k} \le 1, \quad \forall i, \tag{6c}$$

$$\sum_{i=1}^{I} a_{i,j,k} \cdot b_i \le L, \quad \forall j, k, \tag{6d}$$

$$W_i(\mathbf{A}_i, b_i, p_i) \le D_i, \quad \forall i, \tag{6e}$$

$$p_i \le I_{\max}, \quad \forall i, \tag{6f}$$

$$a_{i,j,k} \in \{0,1\}, 0 \le b_i \le L, b_i \in \mathbb{Z}^+, p_i \ge 0, \quad \forall i,j,k. \tag{6g}$$

This is a mixed integer nonlinear programming problem. The access matrix $\mathbf{A}$ consists of $I \times J \times K$ elements and the channel matrix $\mathbf{B}$ consists of $I \times 1$ elements. Considering the combination of these two allocation matrices, there are totally $2^{I \times J \times K + I}$ feasible allocation schemes, which increases exponentially with the number of LEO satellites, MEO satellites and beams. If the power matrix $\mathbf{P}$ is further considered, more feasible schemes exist and constitute a huge feasible space. In fact, the optimization problem is NP-hard, which can hardly be solved by intuitive allocation algorithms [26], [27], [28] when I, J, K are large.

IV. Problem Solving

A. Problem Decomposition

Adopting the block coordinate descent method [29], [30], [31], problem in (6) can be decomposed into two subproblems. One is the access scheduling problem for LEO satellites with given channel matrix $\mathbf{B}$ and power matrix $\mathbf{P}$, which is an integer nonlinear programming. The other is the subchannel-power coordinate allocation problem with given access matrix $\mathbf{A}$, which is a mixed integer nonlinear programming. Adopting Algorithm 1 to iteratively solve subproblems 1 and 2, a suboptimal solution of the original problem in (6) can be obtained. Specifically, Algorithm 2 solves subproblem 1 in Section IV-B, Algorithm 3 solves subproblem 2 in Section IV-C.

(1) Subproblem 1: Access scheduling

$$\max_{\mathbf{A}} \ W(\mathbf{A}, \mathbf{B}, \mathbf{P}) \tag{7a}$$

$$s.t. \sum_{j=1}^{J} \sum_{k=1}^{K} a_{i,j,k} \le 1, \quad \forall i, \tag{7b}$$

$$\sum_{i=1}^{I} a_{i,j,k} \cdot b_i \le L, \quad \forall j,k, \tag{7c}$$

$$W_i(\mathbf{A}_i, b_i, p_i) \le D_i, \quad \forall i, \tag{7d}$$

$$a_{i,j,k} \in \{0,1\}, \quad \forall i,j,k. \tag{7e}$$

(2) Subproblem 2: Subchannel-power coordinate allocation

$$\max_{\mathbf{B},\mathbf{P}} \ W(\mathbf{A}, \mathbf{B}, \mathbf{P}) \tag{8a}$$

$$s.t. \ b_i \cdot p_i \le p_{\max}, \quad \forall i, \tag{8b}$$

$$\sum_{i=1}^{I} a_{i,j,k} \cdot b_i \le L, \quad \forall j,k, \tag{8c}$$

$$W_i(\mathbf{A}_i, b_i, p_i) \le D_i, \quad \forall i, \tag{8d}$$

$$p_i \le I_{\max}, \quad \forall i, \tag{8e}$$

$$0 \le b_i \le L, b_i \in \mathbb{Z}^+, p_i \ge 0, \quad \forall i,j,k. \tag{8f}$$

B. Access Scheduling

It is worth noting that the linear constraint (7c) couples $\mathbf{A}_i$ for different $i \in \mathcal{I}$. Therefore we relax constraint (7c) and derive the corresponding Lagrangian function as:

$$L(\mathbf{A}, \boldsymbol{\lambda}) = \sum_{i=1}^{I} W_i - \sum_{j=1}^{J} \sum_{k=1}^{K} \lambda_{j,k} \left(\sum_{i=1}^{I} a_{i,j,k} \cdot b_i - L \right), \tag{9}$$

where $\boldsymbol{\lambda}$ is the Lagrangian multiplier. Adopting dual decomposition [32], [33], [34], problem (7) can be decomposed as the primal problem (10a) and the dual problem (11a):

$$\max_{\mathbf{A}} \ L(\mathbf{A}, \boldsymbol{\lambda}) \tag{10a}$$

$$s.t. \sum_{j=1}^{J} \sum_{k=1}^{K} a_{i,j,k} \le 1, \quad \forall i, \tag{10b}$$

$$W_i(\mathbf{A}_i, b_i, p_i) \le D_i, \quad \forall i, \tag{10c}$$

$$a_{i,j,k} \in \{0,1\}, \quad \forall i,j,k. \tag{10d}$$

$$\min_{\boldsymbol{\lambda}} \sup_{\mathbf{A}} L(\mathbf{A}, \boldsymbol{\lambda}) \tag{11a}$$

$$s.t. \ \lambda_{j,k} \ge 0, \quad \forall i,j,k. \tag{11b}$$

The Lagrangian function can be further decomposed as:

$$L(\mathbf{A}, \boldsymbol{\lambda}) = \sum_{i=1}^{I} U_i + C, \tag{12}$$

Algorithm 1 Access Scheduling and Subchannel-Power Allocation. (Problem Solving of (6))

Input: $B, L, T, \{d_{i,j} | i \in I, j \in J\}, c, t_0,$ $\left\{a_{i,j,k}^{pre} | i \in I, j \in J, k \in K\right\}, \{h_{i,j,k} | i \in I, j \in J, k \in K\},$ σ^2, $p_{\max}$, $\{D_i | i \in I\}, I_{\max}$

1: **Initialization**: Convergence threshold $\varepsilon_0 = 10^{-3}$, iteration index $r = 0$, initial allocation scheme $\mathbf{A}_0 = \mathbf{0}, \mathbf{B}_0 = \mathbf{0}, \mathbf{P}_0 = \mathbf{0}$
2: **repeat**
3: $r = r + 1$;
4: Solve problem in (7) according to Algorithm 2 and derive $\mathbf{A}_r$;
5: Solve problem in (8) according to Algorithm 3 and derive $\mathbf{B}_r, \mathbf{P}_r$;
6: **until** $\left| 1 - \frac{W(\mathbf{A}_{r-1}, \mathbf{B}_{r-1}, \mathbf{P}_{r-1})}{W(\mathbf{A}_r, \mathbf{B}_r, \mathbf{P}_r)} \right| \le \varepsilon_0$

Output: Access matrix $\mathbf{A}_r$, channel matrix $\mathbf{B}_r$, and power matrix $\mathbf{P}_r$

Algorithm 2 Access Scheduling. (Problem Solving of (7))

Input: Access matrix $\mathbf{A}_{r-1}$, channel matrix $\mathbf{B}_{r-1}$, power matrix $\mathbf{P}_{r-1}$ in the r-th iteration of Algorithm 1; initial step size δ

1: **Initialization**: $\mathbf{A}^0 = \mathbf{A}_{r-1}, \mathbf{B} = \mathbf{B}_{r-1}, \mathbf{P} = \mathbf{P}_{r-1}$, $\boldsymbol{\lambda}^0 = 0, t = 1$
2: **repeat**
3: Update $\mathbf{A}^t$ according to (16) for each $i \in \mathcal{I}$;
4: Update $\boldsymbol{\lambda}^t$ according to (17), where $\delta(t) = \frac{\delta}{t}$;
5: $t = t + 1$;
6: **until** $\mathbf{A}^t = \mathbf{A}^{t-1}$

Output: Access matrix $\mathbf{A}_r = \mathbf{A}^t$

$$U_i\left(\mathbf{A}_i,\boldsymbol{\lambda}\right)=W_i-\sum_{j=1}^{J}\sum_{k=1}^{K}\lambda_{j,k}\cdot a_{i,j,k}\cdot b_i, \tag{13}$$

$$C=L\sum_{j=1}^{J}\sum_{k=1}^{K}\lambda_{j,k}. \tag{14}$$

According to Lagrangian dual method, $\mathbf{A}$ is updated in the t-th iteration to solve problem (10a):

$$\mathbf{A}^{t+1}=\arg\max_{\mathbf{A}}\sum_{i=1}^{I}U_i+C. \tag{15}$$

For any given i, U_i is only related to $\mathbf{A}_i=\{a_{i,j,k}|j\in\mathcal{J},k\in\mathcal{K}\}$, and C is independent of $\mathbf{A}$. Therefore, (15) can be equivalently decomposed as:

$$\mathbf{A}_i^{t+1}=\arg\max_{\mathbf{A}_i\in\mathcal{A}_i}U_i, \tag{16}$$

where $\mathcal{A}_i=\{\mathbf{A}_i|\sum_{j=1}^{J}\sum_{k=1}^{K}a_{i,j,k}\le 1;\ W_i\left(\mathbf{A}_i,b_i,p_i\right)\le D_i;\ a_{i,j,k}\in\{0,1\},\forall j,k\}$. Here we define $\mathcal{A}_i^0=\{\mathbf{A}_i|\sum_{j=1}^{J}\sum_{k=1}^{K}a_{i,j,k}\le 1;\ a_{i,j,k}\in\{0,1\},\forall j,k\}$. Evidently, there are $J\times K+1$ elements in $\mathcal{A}_i^0$, and $\mathcal{A}_i\subset\mathcal{A}_i^0$. Therefore, there are no more than $J\times K+1$ elements in $\mathcal{A}_i$, which means (16) can be easily solved by exhaustive search.

Adopting the subgradient descent method to solve dual problem (11a), the Lagrangian multipliers are iteratively updated as:

$$\lambda_{j,k}^{t+1}=\left[\lambda_{j,k}^{t}+\delta\left(t\right)\cdot\left(\sum_{i=1}^{I}a_{i,j,k}\cdot b_i-L\right)\right]^{+}, \tag{17}$$

where $[*]^{+}=\max\left(*,0\right)$, $\delta\left(t\right)$ is the step sizes in the t-th iteration. Algorithm 2 shows the overall problem solving process for (7).

C. Subchannel-Power Coordinate Allocation

Intuitively, the objective function (8a) and constraints (8b), (8d), (8e) increase monotonically with p_i. Therefore, the optimal solution satisfies:

$$p_i=\min\left\{\frac{p_{\max}}{b_i+\Delta},I_{\max},G_i\left(b_i\right)\right\}, \tag{18}$$

where $\Delta\to 0^{+}$, and $p_i=G_i\left(b_i\right)$ is the implicit function satisfying $W_i\left(p_i,b_i\right)=D_i$. Substituting (18) into problem in (8), the optimization problem only related to channel matrix $\mathbf{B}$ can be obtained as:

$$\max_{\mathbf{B}}\ \sum_{j=1}^{J}\sum_{k=1}^{K}W_{j,k} \tag{19a}$$

$$s.t.\ \sum_{i\in\mathcal{I}_{j,k}}b_i\le L,\quad\forall j,k, \tag{19b}$$

$$0\le b_i\le L,b_i\in\mathbb{Z}^{+},\quad\forall i, \tag{19c}$$

where $\mathcal{I}_{j,k}=\{i|a_{i,j,k}=1\}$. Since $\sum_{j=1}^{J}\sum_{k=1}^{K}a_{i,j,k}\le 1$, we have $\mathcal{I}_{j_1,k_1}\cap\mathcal{I}_{j_2,k_2}=\emptyset$ for any $\{j_1,k_1\}\ne\{j_2,k_2\}$, which means $W_{j,k}$ is only determined by $\{b_i|i\in\mathcal{I}_{j,k}\}$. Therefore, problem in (19) can be decomposed into $J\times K$ independent subproblems:

$$\max_{\{b_i|i\in\mathcal{I}_{j,k}\}}\ W_{j,k} \tag{20a}$$

$$s.t.\ \sum_{i\in\mathcal{I}_{j,k}}b_i\le L, \tag{20b}$$

$$0\le b_i\le L,\quad b_i\in\mathbb{Z}^{+},\ \forall i\in\mathcal{I}_{j,k}. \tag{20c}$$

Considering that only L_0 subchannels are used, the optimization problem $Q_{j,k}\left(L_0\right)$ is defined on the basis of problem in (20):

$$\max_{\{b_i|i\in\mathcal{I}_{j,k}\}}\ W_{j,k} \tag{21a}$$

$$s.t.\ \sum_{i\in\mathcal{I}_{j,k}}b_i\le L_0, \tag{21b}$$

$$0\le b_i\le L_0,\quad b_i\in\mathbb{Z}^{+},\ \forall i\in\mathcal{I}_{j,k}. \tag{21c}$$

With careful proofs shown in the appendices, Theorem 1 to 6 could be derived.

Theorem 1: $\Delta W_{i,j,k}(b_i)\le\Delta W_{i,j,k}(b_i-1)$ *holds for any* $i\in\mathcal{I}_{j,k}$, *where* $\Delta W_{i,j,k}(b_i)=W_{i,j,k}(b_i+1)-W_{i,j,k}(b_i)$.

Theorem 2: If $\{b_i^{\star}|i\in\mathcal{I}_{j,k}\}$ *is the optimal solution of problem in (20), then for any* $i_1,i_2\in\mathcal{I}_{j,k}$ *and* $1\le n\le L$, *we have* $\Delta W_{i_1,j,k}(b_{i_1}^{\star}-n)\ge\Delta W_{i_2,j,k}(b_{i_2}^{\star})$ *and* $\Delta W_{i_1,j,k}(b_{i_1}-n)\ge 0$.

Theorem 3: For any $i_1,i_2\in\mathcal{I}_{j,k}$ *and* $1\le n\le L$, *if* $\{b_i^{\star}|i\in\mathcal{I}_{j,k}\}$ *satisfies* $\Delta W_{i_1,j,k}(b_{i_1}^{\star}-n)\ge\Delta W_{i_2,j,k}(b_{i_2}^{\star})$, $\Delta W_{i_1,j,k}(b_{i_1}^{\star}-n)\ge 0$ *and* $\sum_{i\in\mathcal{I}_{j,k}}b_i^{\star}=L$, *then it is the optimal solution of problem in (20).*

Theorem 4: Given that the optimal solution $\{b_i^{\star}|i\in\mathcal{I}_{j,k}\}$ *of problem* $Q_{j,k}\left(L_0\right)$ *is on the constraint boundary of (20a), that is* $\sum_{i\in\mathcal{I}_{j,k}}b_i^{\star}=L_0$. *If* $\Delta W_{i_0,j,k}\left(b_{i_0}^{\star}\right)<0$, *where* $i_0=\arg\max_i\Delta W_{i,j,k}\left(b_i^{\star}\right)$, *then the optimal solution of problem* $Q_{j,k}\left(L_0+1\right)$ *is* $\{b_i^{\star}|i\in\mathcal{I}_{j,k}\}$.

Theorem 5: Given that the optimal solution $\{b_i^{\star}|i\in\mathcal{I}_{j,k}\}$ *of problem* $Q_{j,k}\left(L_0\right)$ *is on the constraint boundary of (20a), that is* $\sum_{i\in\mathcal{I}_{j,k}}b_i^{\star}=L_0$. *If* $\Delta W_{i_0,j,k}\left(b_{i_0}^{\star}\right)\ge 0$, *where* $i_0=\arg\max_i\Delta W_{i,j,k}\left(b_i^{\star}\right)$, *then the optimal solution of problem* $Q_{j,k}\left(L_0+1\right)$ *is* $\left\{b_i^{+}|i\in\mathcal{I}_{j,k}\right\}=\{b_i^{\star}|i\in\mathcal{I}_{j,k}/\{i_0\}\}\cup\left\{b_{i_0}^{\star}+1\right\}$.

Theorem 6: If the optimal solution $\{b_i^{\star}|i\in\mathcal{I}_{j,k}\}$ *of problem* $Q_{j,k}\left(L_0\right)$ *is not on the constraint boundary of (20a), that is* $\sum_{i\in\mathcal{I}_{j,k}}b_i^{\star}<L_0$, *then the optimal solution of problem* $Q_{j,k}\left(L_0+1\right)$ *is* $\{b_i^{\star}|i\in\mathcal{I}_{j,k}\}$.

Based on the theorems above, we progressively solve problem in (19). Firstly, the optimal solution of $Q_{j,k}\left(1\right)$ is derived directly. Then according to Theorem 4,5 and 6, the optimal solution of $Q_{j,k}\left(L_0+1\right)$ is progressively derived from the optimal solution of $Q_{j,k}\left(L_0\right)$ until L subchannels are allocated to LEO satellites in L rounds. Furthermore, the $J\times K$ independent problems $\{Q_{j,k}\left(L\right)|j\in\mathcal{J},k\in\mathcal{K}\}$ can be identically solved in the above process to derive the optimal subchannel-power coordinate allocation scheme. The detailed algorithm is shown in Algorithm 3.

Algorithm 3 Subchannel-Power Coordinate Allocation. (Problem Solving of (8))

Input: Access matrix $\mathbf{A}_r$ in the r-th iteration of Algorithm 1

for $j = 1$ to J **do**
  for $k = 1$ to K **do**
    Initialize $b_i = 0$ for any $i \in \mathcal{I}_{j,k}$;
    for $l = 1$ to L **do**
      if $\sum \{b_i | i \in \mathcal{I}_{j,k}\} < l - 1$ **then**
        Break;
      else
        Set $i_0 = \arg\max_i \Delta W_{i,j,k}(b_i)$;
        if $\Delta W_{i_0,j,k}(b_{i_0}) < 0$ **then**
          Continue;
        else
          $b_{i_0} = b_{i_0} + 1$;
        end if
      end if
    end for
  end for
end for
for $i = 1$ to I **do**
  $p_i = \min\left\{\frac{p_{\max}}{b_i + \Delta}, I_{\max}, G_i(b_i)\right\}$;
end for

Output: Channel matrix $\mathbf{B}_r$ and power matrix $\mathbf{P}_r$

D. Convergence Analysis

Considering using Algorithm 1 to solve problem in (6), we assumes that $\mathbf{A}_{r-1}, \mathbf{B}_{r-1}, \mathbf{P}_{r-1}$ are the solutions of subproblems in (7) and (8) for the $r-1$-th iteration. In the r-th iteration, we first solve subproblem in (7) to derive $\mathbf{A}_r$. By solving problem in (7), the objective value of the locally optimal solution $\mathbf{A}_r$ is not less than that of the original solution $\mathbf{A}_{r-1}$:

$$W(\mathbf{A}_{r-1}, \mathbf{B}_{r-1}, \mathbf{P}_{r-1}) \leq W(\mathbf{A}_r, \mathbf{B}_{r-1}, \mathbf{P}_{r-1}). \quad (22)$$

Then, the optimal solutions $\mathbf{B}_r, \mathbf{P}_r$ are obtained by solving subproblem in (8), which satisfies:

$$W(\mathbf{A}_r, \mathbf{B}_{r-1}, \mathbf{P}_{r-1}) \leq W(\mathbf{A}_r, \mathbf{B}_r, \mathbf{P}_r). \quad (23)$$

Therefore, we have

$$W(\mathbf{A}_{r-1}, \mathbf{B}_{r-1}, \mathbf{P}_{r-1}) \leq W(\mathbf{A}_r, \mathbf{B}_r, \mathbf{P}_r). \quad (24)$$

After each iteration, the objective value of problem in (6) increases monotonically. Meanwhile, since the system resources are limited, the upper bound exists for the transmitted data amount, which is the objective value. Therefore, Algorithm 1 converges and can at least obtain a locally optimal solution.

E. Complexity Analysis

Firstly, we analyze the complexity of Algorithm 2 for access scheduling. In step 3, obtaining the maximum $\mathbf{A}_i^{t+1}$ needs to search $J \times K + 1$ elements in $\mathcal{A}_i$, therefore obtaining the maximum $\mathbf{A}^{t+1}$ has the complexity of $O(IJK)$. In step 4, updating each $\lambda_{j,k}^{t+1}$ has the complexity of $O(I)$ and updating each μ_i^{t+1} has the complexity of $O(JK)$, therefore updating $\boldsymbol{\lambda}^t$ and $\boldsymbol{\mu}^t$ both have the complexity of $O(IJK)$. Consequently, the complexity in each iteration of Algorithm 2 is $O(IJK)$ and the overall complexity of Algorithm 2 is $O(IJKM_1)$, where M_1 is the maximum number of iterations.

Secondly, we analyze the complexity of Algorithm 3 for subchannel-power allocation. The algorithm has 3 nested loops with lengths of J, K and L. Since calculating $i_0 = \arg\max_i \Delta W_{i,j,k}(b_i)$ in step 8 needs to search I elements, the overall complexity of Algorithm 3 is $O(IJKL)$.

Finally, we analyze the complexity of Algorithm 1 for access scheduling and subchannel-power allocation. In each iteration, Algorithm 2 and 3 are implemented. Therefore, the overall complexity of Algorithm 1 is $O(IJKM_2(M_1 + L))$, where M_2 is the maximum number of iterations. Evidently, the overall complexity is linearly correlated with I, J, K, L, which means the proposed algorithms are computationally affordable.

V. Upper Bound Performance Analysis

Techniques that deal with non-convexity are adopted for problem solving, which include the block coordinate decent method for problem decomposition and the successive optimization technique for non-convexity approximation. Evidently, these techniques introduce performance gap between the solution of our proposed algorithm and the theoretically optimal solution, which needs further analysis. In this section, we first relax the constrains of problem (6) to formulate the upper bound problem. Then by optimally solve the upper bound problem, the upper bound performance of problem (6) can be derived and compared with the performance of our proposed algorithm, so as to evaluate the performance gap.

A. Formulation of the Upper Bound Problem

First, we define $b_i = \sum_{j=1}^{J}\sum_{k=1}^{K} b_{i,j,k}$ and extend the channel matrix $\mathbf{B}$ to the dimension of $I \times J \times K$. Then, we relax constraints (6c) and (6e) of problem in (6) to get the upper bound problem in (25). Specifically, the upper bound problem in (25) allows each LEO satellite to simultaneously access multiple beams of multiple MEO satellites, and assumes the maximum cached data amount of each LEO satellite as infinite. Obviously, the feasible region of problem in (6) is the subset of that of problem in (25), which means that the optimal solution of problem in (25) is the upper bound of that of problem in (6).

$$\max_{\mathbf{A},\mathbf{B},\mathbf{P}} \sum_{i=1}^{I}\sum_{j=1}^{J}\sum_{k=1}^{K} W_{i,j,k}(\mathbf{A}, \mathbf{B}, \mathbf{P}) \quad (25a)$$

$$s.t. \sum_{j=1}^{J}\sum_{k=1}^{K} b_{i,j,k} \cdot p_i \leq p_{\max}, \quad \forall i, \quad (25b)$$

$$\sum_{i=1}^{I} a_{i,j,k} \cdot b_{i,j,k} \leq L, \quad \forall j, k, \quad (25c)$$

$$p_i \leq I_{\max}, \quad \forall i, \quad (25d)$$

$$a_{i,j,k} \in \{0,1\},\ b_{i,j,k} \geq 0,\ b_{i,j,k} \in \mathbb{Z}^+,$$
$$p_i \geq 0, \quad \forall i,j,k. \tag{25e}$$

Since the objective value W increases monotonically with the increase of p_i, the optimal solution necessarily meets:

$$p_i = \min\left\{\frac{p_{\max}}{b_i+\Delta}, I_{\max}\right\}, \tag{26}$$

where $\Delta \to 0^+$. The above formula is substituted into the upper bound problem in (25), which derives:

$$\max_{\mathbf{A},\mathbf{B}} \sum_{i=1}^{I}\sum_{j=1}^{J}\sum_{k=1}^{K} W_{i,j,k}(\mathbf{A},\mathbf{B},\mathbf{P}) \tag{27a}$$

$$s.t. \sum_{i=1}^{I} a_{i,j,k}\cdot b_{i,j,k} \leq L, \quad \forall j,k, \tag{27b}$$

$$a_{i,j,k} \in \{0,1\}, \quad b_{i,j,k} \geq 0,\ b_{i,j,k} \in \mathbb{Z}^+,\ \forall i,j,k, \tag{27c}$$

where

$$W_{i,j,k} = \frac{B}{L}\cdot\left(T - \left(\frac{d_{i,j}}{c}+t_0\right)\cdot\left(a_{i,j,k} - a_{i,j,k}^{pre}\right)\right)\cdot a_{i,j,k} \cdot b_{i,j,k}\cdot\log_2\left(1+\frac{|h_{i,j,k}|^2\cdot\min\left\{\frac{p_{\max}}{b_i+\Delta}, I_{\max}\right\}}{\sigma^2}\right). \tag{28}$$

Theorem 7: There must exist an optimal solution of problem in (27), which satisfies $a^\star_{i,j,k}=1$ for any $i\in I, j\in J, k\in K$.

According to Theorem 7, we only consider the optimal solutions satisfying $a^\star_{i,j,k}=1$ for any $i\in I, j\in J, k\in K$, then problem in (27) can be simplified as:

$$\max_{\mathbf{B}} \sum_{i=1}^{I}\sum_{j=1}^{J}\sum_{k=1}^{K} W_{i,j,k}(\mathbf{A},\mathbf{B},\mathbf{P}) \tag{29a}$$

$$s.t. \sum_{i=1}^{I} b_{i,j,k} \leq L, \quad \forall j,k, \tag{29b}$$

$$b_{i,j,k} \geq 0, \quad b_{i,j,k} \in \mathbb{Z}^+,\ \forall i,j,k, \tag{29c}$$

where

$$W_{i,j,k} = \frac{B}{L}\cdot\left(T - \left(\frac{d_{i,j}}{c}+t_0\right)\cdot\left(1 - a_{i,j,k}^{pre}\right)\right)\cdot b_{i,j,k} \cdot\log_2\left(1+\frac{|h_{i,j,k}|^2\cdot\min\left\{\frac{p_{\max}}{b_i+\Delta}, I_{\max}\right\}}{\sigma^2}\right). \tag{30}$$

B. Globally Optimal Solution of the Upper Bound Problem

We set the objective value corresponding to the solution that does not meet constraint (29b) as negative infinite, limit the number of overall allocated subchannels to no more than M, and define problem $Q(M)$ as:

$$\max_{\mathbf{B}} \quad W(\mathbf{A},\mathbf{B},\mathbf{P}) \tag{31a}$$

$$s.t. \quad \sum_{i=1}^{I}\sum_{j=1}^{J}\sum_{k=1}^{K} b_{i,j,k} \leq M, \tag{31b}$$

$$b_{i,j,k} \geq 0, b_{i,j,k} \in \mathbb{Z}^+, \quad \forall i,j,k, \tag{31c}$$

where

$$W = \begin{cases} \sum_{i=1}^{I}\sum_{j=1}^{J}\sum_{k=1}^{K} W_{i,j,k} \ if \ \sum_{i=1}^{I} b_{i,j,k} \leq L \ for\ any\ j,k \\ -\infty \qquad\qquad else \end{cases} \tag{32}$$

Obviously, problem in (29) is equivalent to $Q(L\cdot J\cdot K)$. With careful proof shown in the appendix, Theorem 8 could be derived.

Theorem 8: $\Delta W(b_{i,j,k}) \leq \Delta W(b_{i,j,k}-1)$ holds for any $(i,j,k)\in I\times J\times K$, where $\Delta W(b_{i,j,k}) = W(b_{i,j,k}+1) - W(b_{i,j,k})$.

According to the objective function properties illustrated in Theorem 1 and Theorem 8, and the constraints defined in (31b) and (20a), we can find that problem in (31) is similar to problem in (20). Similarly, Theorem 9 to 11 hold for problem in (31), and their proofs are omitted since they are basically the same as the proofs of Theorem 4 to Theorem 6.

Theorem 9: If the optimal solution $\{b^\star_{i,j,k}|\,(i,j,k) \in I\times J\times K\}$ of $Q(M)$ satisfies $\sum_{i=1}^{I}\sum_{j=1}^{J}\sum_{k=1}^{K} b^\star_{i,j,k} = M$, we define $(i_0,j_0,k_0) = \arg\max_{(i,j,k)\in I\times J\times K} \Delta W(b^\star_{i,j,k})$. If $\Delta W(b^\star_{i_0,j_0,k_0}) < 0$, then the optimal solution of $Q(M+1)$ is $\{b^\star_{i,j,k}|\,(i,j,k)\in I\times J\times K\}$.

Theorem 10: If the optimal solution $\{b^\star_{i,j,k}|\,(i,j,k) \in I\times J\times K\}$ of $Q(M)$ satisfies $\sum_{i=1}^{I}\sum_{j=1}^{J}\sum_{k=1}^{K} b^\star_{i,j,k} = M$, we define $(i_0,j_0,k_0) = \arg\max_{(i,j,k)\in I\times J\times K} \Delta W(b^\star_{i,j,k})$. If $\Delta W(b^\star_{i_0,j_0,k_0}) \geq 0$, then the optimal solution of $Q(M+1)$ is $\{b^+_{i,j,k}|\,(i,j,k)\in I\times J\times K\} = \{b^\star_{i,j,k}|\,(i,j,k)\in I\times J\times K/(i_0,j_0,k_0)\}\bigcup\{b^\star_{i_0,j_0,k_0}+1\}$.

Theorem 11: If the optimal solution $\{b^\star_{i,j,k}|\,(i,j,k)\in I\times J\times K\}$ of $Q(M)$ satisfies $\sum_{i=1}^{I}\sum_{j=1}^{J}\sum_{k=1}^{K} b^\star_{i,j,k} < M$, then the optimal solution of $Q(M+1)$ is $\{b^\star_{i,j,k}|(i,j,k)\in I\times J\times K\}$.

Similar to Algorithm 3, problems $Q(1),\ldots,Q(L\cdot J\cdot K)$ can be progressively solved according to Theorems 9, 10 and 11. In this way, the globally optimal solution of the upper bound problem in (31) can be obtained, whose performance serves as the upper bound of the original problem in (6).

VI. Numerical Simulation

A. System Architecture and Parameters for Simulation

The MEO constellation adopts the rose-typed configuration, which is composed of 8 satellites distributed in 8 symmetrical orbital planes. Specifically for MEO-1 to MEO-8, the orbital periods are 12 hours, the semimajor axes are 26560 km, the eccentricities are 0, the inclinations are 53.13 deg, the arguments of perigee are 0 deg, the right ascensions of the ascending node are (0, 45, 90, 135, 180, 225, 270, 315) deg, the mean anomalies are (218, 128, 38, 308, 218, 128, 38, 308) deg. The LEO satellite constellation is composed of 1,600 satellites of Starlink [35], which locate at orbital planes with the inclinations of 53 deg, the eccentricities of 0 and the

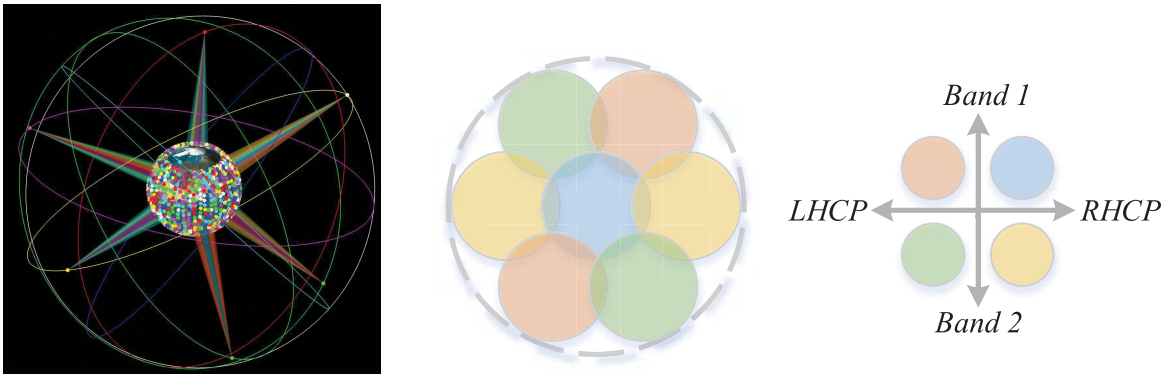

(a) The spatial topology of the LEO and MEO constellations.

(b) Beams of the MEO satellites.

Fig. 2. Configuration of the satellite constellations and beams.

altitudes of 550 km. The spatial topology of the LEO and MEO constellations is shown in Fig. 2(a).

In order to receive telemetry data from the LEO satellites, each MEO satellite is equipped with 7 directional beams. Referring to [36], the beam spatial relationship is shown in Fig. 2, and the central blue beam points to the earth center. In order to avoid interference between beams, adjacent beams adopt different polarization modes and frequency bands. Specifically, according to different polarization modes and frequency bands, beams can be divided into four categories with colors of blue, green, red and yellow. The red and green beams adopt the left-handed circular polarization, while the yellow and blue beams adopt the right-handed circular polarization. The red and blue beams occupy Band 1, while the green and yellow beams occupy Band 2. Therefore, there is no interference between any two adjacent beams. In addition, for non-adjacent beams with the same polarization mode and frequency band, since they are spatially isolated, it can be approximately considered that there is no interference between beams with limiting the transmission power.

Based on the above LEO and MEO constellations architecture and beams configuration, we further define the detailed simulation parameters as shown in Table I. An orbital period of the LEO satellite can be divided into multiple time slots, and the resource allocation algorithm is executed for each time slot to obtain the resource allocation scheme. By analyzing the transmitted data amount of the networked telemetry system in each time slot and an orbital period, the performance of the resource allocation algorithm is evaluated.

TABLE I
SIMULATION PARAMETERS

Parameter	Value
Length of time slot	0.5 s
Orbital period of LEO satellites	5735 s
Signal frequency band	X-band
Bandwidth of each beam of MEO satellites	1 MHz
Number of subchannels of each beam of MEO satellites	1000
Half beam width of MEO satellites	3 deg
G/T of receiving antennas of MEO satellites [37]	0 dB/K
Noise temperature of MEO satellite receivers	300 K
Maximum total transmission power of LEO satellites	10 W
Maximum transmission power on each subchannel of LEO satellites	1 W
Antenna transmission gain of LEO satellites	0 dB
Generation rate of telemetry data of LEO satellites	10 kbps
Handover time of LEO satellites	2 ms

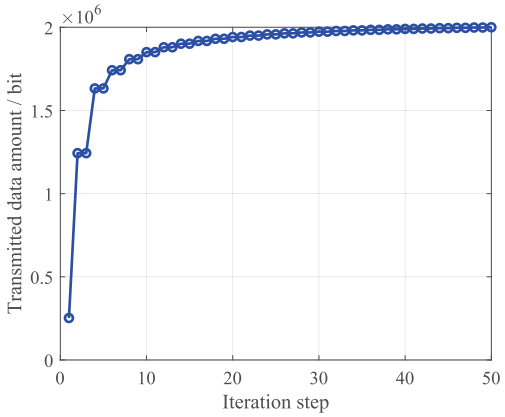

Fig. 3. The convergence process of Algorithm 1.

B. Performance Analysis and Comparison

Firstly, the convergence of Algorithm 1 is verified, with the convergence process shown in Fig. 3. The transmitted data amount of the system increases iteratively and tends to be stable with about 20 iterations.

In order to intuitively and visually show the resource allocation schemes, we demonstrate the access scheduling, the subchannel allocation and the power allocation of MEO-1 in Fig. 4 and Table II. Since the resource allocation schemes of other MEO satellites are similar, they are not respectively demonstrated in detail here. Specifically, in the direction from the MEO satellite to the earth center, Fig. 4 shows the MEO beam coverage and the LEO satellites accessing the beams. Large circles represent coverages of MEO beams, while small circles represent LEO satellites. Each LEO satellite accesses the MEO beam in the same color. In terms of the access scheduling, the numbers of LEO satellites in different MEO beams are balanced, so that resources in different MEO beams

TABLE II
DEMONSTRATION OF ALLOCATION SCHEME FOR MEO-1

LEO satellite	Channel gain /dB	Accessed MEO beam	Subchannel number	Transmission power /W	LEO satellite	Channel gain /dB	Accessed MEO beam	Subchannel number	Transmission power /W
1	-173.44	1	220	0.0454	2	-171.67	1	331	0.0302
3	-173.81	1	188	0.0531	4	-172.70	1	261	0.0383
5	-173.18	2	296	0.0337	6	-171.95	2	393	0.0254
7	-172.97	2	311	0.0321	8	-174.07	3	207	0.0483
9	-171.78	3	351	0.0284	10	-174.46	3	189	0.0529
11	-173.20	3	253	0.0395	12	-172.79	4	248	0.0403
13	-173.18	4	226	0.0442	14	-172.01	4	296	0.0337
15	-173.12	4	230	0.0434	16	-172.38	5	364	0.0274
17	-173.47	5	282	0.0354	18	-172.50	5	354	0.0282
19	-173.77	6	222	0.0450	20	-173.87	6	217	0.0460
21	-173.21	6	253	0.0395	22	-172.35	6	308	0.0324
23	-174.43	7	188	0.0531	24	-171.94	7	334	0.0299
25	-172.51	7	293	0.0341	26	-174.50	7	185	0.0540

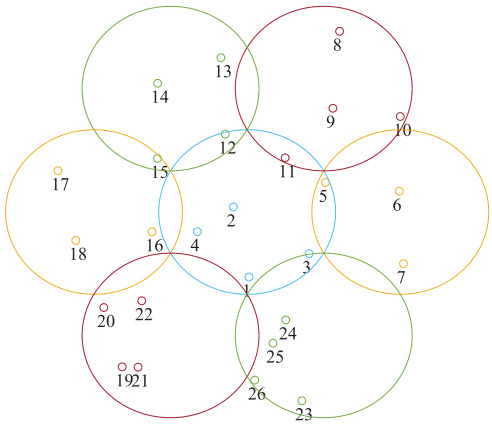

Fig. 4. Demonstration of allocation scheme for MEO-1.

can be fully utilized. For example, although LEO-11 is closer to beam-1, it still accesses beam-3 because there are already 4 LEO satellites served by beam-1. In terms of the channel allocation, the LEO satellites with higher channel gain are allocated with more channels, so that channel resources can be fully utilized. For example, LEO-5, LEO-6, LEO-7 within beam-2 can be sorted in ascending order of channel gain as LEO-6 $>$ LEO-7 $>$ LEO-5, which is exactly in the same ascending order of subchannel number. In terms of the power allocation, the transmission power is maximized to reach the constraint of power limitation, so that power resources can be fully utilized. For example, LEO-8 to LEO-11 within beam-3 promote the transmission power in each subchannel to reach the maximum power limitation of 10 W.

In order to further verify the performance of the proposed algorithm, the following comparative schemes are considered in this paper:

Comparative Algorithm 1: Based on the block coordinate descent method in [38], the optimization problem is decomposed into three subproblems: the access scheduling, the subchannel allocation and the power allocation. The above three subproblems are solved iteratively to obtain the overall resource allocation scheme.

Comparative Algorithm 2: Based on time division multiplexing, each beam is accessed by the LEO satellite with the lowest attenuation in each time slot. And the LEO satellite send data with the maximum transmission power using all subchannels in the beam.

The bandwidth of each beam of MEO satellites, the half beam width of MEO satellites, the maximum total transmission power of LEO satellites and the generation rate of telemetry data of LEO satellites are respectively changed to observe their influences on the transmitted data amount of the whole telemetry system which is averaged by time slots during one orbital period.

First, we comprehensively compare the performances of the three algorithms and the upper bound. According to Fig. 5(a) to 5(e), the performance of the proposed algorithm approximates that of the upper bound, which indicates that the suboptimal solution obtained by the proposed algorithm gets very close to the globally optimal solution of problem in (6). In addition, the performance of the proposed algorithm is better than that of Comparative Algorithm 1. This is because the proposed algorithm decomposes the resource allocation problem into two subproblems, and Comparative Algorithm 1 decomposes the resource allocation problem into three subproblems. Problem decomposition with the block coordinate descent method can reduce the complexity of problem solving, but at the expense of limiting the direction of the single-step iteration. Therefore, the more subproblems are decomposed into, the less possibly the solution will converge to the optimum. Besides, the performance of the proposed algorithm is better than that of Comparative Algorithm 2. This is because the LEO satellite with the lowest attenuation connected to each beam is allocated with too many subchannels, which renders the transmission capacity almost saturated for the single LEO satellite.

Then, we detailedly analyse the performances of the three algorithms and the upper bound in each simulation.

Fig. 5(a) illustrates the transmitted data amounts during 7 orbital periods of the upper bound and the three algorithms. Specifically, the transmitted data amounts of the upper bound, the proposed algorithm and Comparative Algorithm 1 fluctuate substantially, while the transmitted data amount of Comparative Algorithm 2 fluctuates slightly. This is because with the relative motion of the LEO and MEO satellites, the channel attenuations in different time slots would fluctuate greatly.

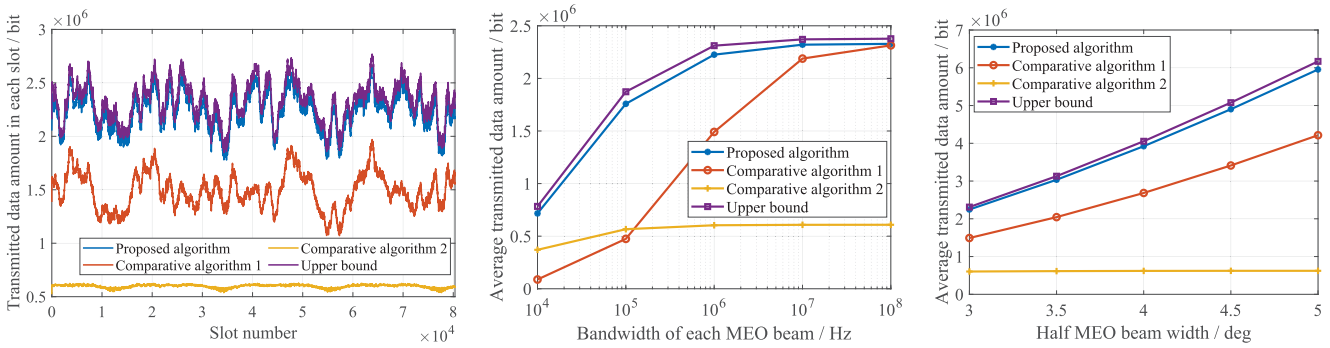

(a) Transmitted data amounts during 7 orbital periods. (b) Average transmitted data amounts under different bandwidths of MEO beams. (c) Average transmitted data amounts under different half beam widths.

(d) Average transmitted data amounts under different maximum transmission powers. (e) Average transmitted data amounts under different data generation rates of LEO satellites.

Fig. 5. Performance comparison of different algorithms.

In Comparative Algorithm 2, only the LEO satellite with the lowest channel attenuation transmits data in each time slot, which is usually located in the center of the beam coverage area and keeps a stable spatial relative position with the MEO satellite. Therefore, the channel attenuation is slightly affected by the relative motion of the satellites.

Fig. 5(b) shows that as the bandwidth of each beam of MEO satellites increases, the average transmitted data amounts per time slot of all algorithms increase, and the differences of the average transmitted data amounts of the upper bound, the proposed algorithm and Comparative Algorithm 1 decrease. This is because as the bandwidth increases, the bandwidth resources are no longer in shortage. The performance loss of suboptimal access scheduling and power allocation scheme can be compensated by allocation of extensive bandwidth. Therefore, the performance gap between the optimal and suboptimal solutions on resource allocation decreases.

Fig. 5(c) shows that as the half beam width of MEO satellites increases, the average transmitted data amounts per time slot of the upper bound, the proposed algorithm and Comparative Algorithm 1 increase, while the average transmitted data amount of Comparative Algorithm 2 remains unchanged. This is because as the beam width increases, the number of LEO satellites covered by the beam increases, so the idle subchannels can be used to a greater extent for the upper bound, the proposed algorithm and Comparative Algorithm 1. In Comparative Algorithm 2, all subchannels are allocated to the LEO satellite with the lowest attenuation in each time slot, so more LEO satellites accessing the beam will not increase the average transmitted data amount.

Fig. 5(d) shows that as the maximum transmission power of LEO satellites increases, the average transmitted data amounts per time slot of the upper bound and all algorithms increase. This is because as the maximum transmission power increases, a higher signal-to-noise ratio and data transmission rate can be achieved.

Fig. 5(e) shows that as the generation rate of telemetry data of LEO satellites increases, the average transmitted data amounts per time slot of all algorithms first increase and then remain unchanged. This is because when the data generation rate is low, the system still remains available resources for transmission of extra data, so a higher data generation rate yields a more adequate utilization of resources and improves the average transmitted data amount. In contrast, when the data generation rate is high, the system no longer has available resources to transmit more data, so a higher data generation rate would not improve the average transmitted data amount.

VII. Conclusion

In order to overcome the defects of the traditional ground-based and GEO-based telemetry systems, the networked telemetry system is considered in this paper, which transmits telemetry data on ISLs of MEO and LEO satellites. This paper formulates the optimization problem to improve the transmitted data amount. For problem solving, the problem is decomposed into the access scheduling subproblem

and the subchannel-power coordinate allocation subproblem using the block coordinate descent method. By iteratively solving the subproblems, the suboptimal resource allocation scheme could be derived. Moreover, this paper formulates the upper bound problem and derives its globally optimal solution, whose performance is the theoretical upper bound of the original resource allocation problem. Finally, the numerical simulations verify that the proposed resource allocation algorithm can effectively improves the transmitted data amount of the networked telemetry system and approximates the upper bound performance. In the future, more complicated resource allocation senario for the networked telemetry system that considers flexible MEO beam steering will be further studied.

APPENDIX

Proof of Theorem 1:

Proof: If $p_i = \frac{p_{\max}}{b_i+\Delta}$, the second derivative of $W_{i,j,k}$ with respect to b_i is always negative, therefore $\Delta W_{i,j,k}(b_i) < \Delta W_{i,j,k}(b_i-1)$. If $p_i = I_{\max}$, the second derivative of $W_{i,j,k}$ with respect to b_i is always zero, therefore $\Delta W_{i,j,k}(b_i) = \Delta W_{i,j,k}(b_i-1)$. If $p_i = G_i(b_i)$, $W_{i,j,k}$ remains unchanged with the increase of b_i, therefore $\Delta W_{i,j,k}(b_i) = \Delta W_{i,j,k}(b_i-1) = 0$.

In conclusion, if $p_i = \min\left\{\frac{p_{\max}}{b_i+\Delta}, I_{\max}, G_i(b_i)\right\}$, $\Delta W_{i,j,k}(b_i) \le \Delta W_{i,j,k}(b_i-1)$ holds for any $i \in \mathcal{I}_{j,k}$. □

Proof of Theorem 2:

Proof: Assuming there exists $i_1, i_2 \in \mathcal{I}_{j,k}$ satisfying $\Delta W_{i_1,j,k}(b^\star_{i_1}-1) < \Delta W_{i_2,j,k}(b^\star_{i_2})$, then we construct the solution in the feasible region as $\left\{b_i^+ | i \in \mathcal{I}_{j,k}\right\} = \left\{b_i^\star | i \in \mathcal{I}_{j,k}/\left\{i_1, i_2\right\}\right\} \cup \left\{b^\star_{i_2}+1\right\} \cup \left\{b^\star_{i_1}-1\right\}$ satisfying $W_{j,k}\left(\left\{b_i^+\right\}\right) > W_{j,k}\left(\left\{b_i^\star\right\}\right)$, which contradicts with the fact that $\left\{b_i^\star | i \in \mathcal{I}_{j,k}\right\}$ is the optimal solution of problem in (20). Therefore, the assumption is invalid, which means that $\Delta W_{i_1,j,k}(b^\star_{i_1}-1) \ge \Delta W_{i_2,j,k}(b^\star_{i_2})$ holds for any $i_1, i_2 \in \mathcal{I}_{j,k}$. Furthermore, according to Theorem 1, we have $\Delta W_{i_1,j,k}(b^\star_{i_1}-n) \ge \Delta W_{i_2,j,k}(b^\star_{i_2})$ for any $1 \le n \le L$.

Assuming there exists $i_1 \in \mathcal{I}_{j,k}$ satisfying $\Delta W_{i_1,j,k}(b^\star_{i_1}-1) < 0$, then we construct the solution in the feasible region as $\left\{b_i^+ | i \in \mathcal{I}_{j,k}\right\} = \left\{b_i^\star | i \in \mathcal{I}_{j,k}/\left\{i_1\right\}\right\} \cup \left\{b^\star_{i_1}-1\right\}$, which satisfies $W_{j,k}\left(\left\{b_i^+\right\}\right) > W_{j,k}\left(\left\{b_i^\star\right\}\right)$ and contradicts with the fact that $\left\{b_i^\star | i \in \mathcal{I}_{j,k}\right\}$ is the optimal solution of problem in (20). Therefore, the assumption is invalid, which means $\Delta W_{i_1,j,k}(b_{i_1}-1) \ge 0$ holds for any $i_1, i_2 \in \mathcal{I}_{j,k}$. Furthermore, according to Theorem 1, $\Delta W_{i_1,j,k}(b_{i_1}-n) \ge 0$ holds for any $1 \le n \le L$. □

Proof of Theorem 3:

Proof: $W_{j,k}$ can be decomposed as $W_{j,k} = \sum\limits_{i\in\mathcal{I}_{j,k}} W_{i,j,k} = \sum\limits_{i\in\mathcal{I}_{j,k}} \sum\limits_{m=0}^{b_i-1} \Delta W_{i,j,k}(m)$. Therefore, the maximum value of the objective function satisfies

$$\begin{aligned}\max_{\{b_i|i\in\mathcal{I}_{j,k}\}} W_{j,k} &= \max_{\{b_i|i\in\mathcal{I}_{j,k}\}} \sum_{i\in\mathcal{I}_{j,k}} \sum_{m=0}^{b_i-1} \Delta W_{i,j,k}(m) \\ &\le \sum \left\{ \max\nolimits_{i\in\mathcal{I}_{j,k}, 0\le m\le L-1}^{L} \left[\Delta W_{i,j,k}(m)\right]^+ \right\}, \end{aligned} \tag{33}$$

where $\max_L(*)$ represents the first L maximum values, $[*]^+$ is equivalent to $\max(*, 0)$. Considering Theorem 1 and the given condition that for any $i_1, i_2 \in \mathcal{I}_{j,k}$ and $1 \le n \le L$, the solution $\left\{b_i^\star | i \in \mathcal{I}_{j,k}\right\}$ satisfies $\Delta W_{i_1,j,k}(b^\star_{i_1}-n) \ge \Delta W_{i_2,j,k}(b^\star_{i_2})$, we derive that $\Delta W_{i_1,j,k}(b^\star_{i_1}-n_1) \ge \Delta W_{i_2,j,k}(b^\star_{i_2}+n_2)$ holds for any $i_1, i_2 \in \mathcal{I}_{j,k}$ and $1 \le n_1 \le L, 0 \le n_2 \le L$.

And since $\sum\limits_{i\in\mathcal{I}_{j,k}} b_i^\star = L$, we have

$$\begin{aligned} W_{j,k}\left(\left\{b_i^\star\right\}\right) &= \sum_{i\in\mathcal{I}_{j,k}} \sum_{m=0}^{b_i^\star-1} \Delta W_{i,j,k}(m) \\ &= \sum \left\{ \max\nolimits_{i\in\mathcal{I}_{j,k}, 0\le m\le L-1}^{L} \Delta W_{i,j,k}(m) \right\}. \end{aligned} \tag{34}$$

And since $\Delta W_{i_1,j,k}(b^\star_{i_1}-n) \ge 0$, we have

$$\begin{aligned} &\sum \left\{ \max\nolimits_{i\in\mathcal{I}_{j,k}, 0\le m\le L-1}^{L} \left(\Delta W_{i,j,k}(m)\right) \right\} \\ &\quad = \sum \left\{ \max\nolimits_{i\in\mathcal{I}_{j,k}, 0\le m\le L-1}^{L} \left[\Delta W_{i,j,k}(m)\right]^+ \right\}, \end{aligned} \tag{35}$$

$$W_{j,k}\left(\left\{b_i^\star\right\}\right) \ge \max_{\{b_i|i\in\mathcal{I}_{j,k}\}} W_{j,k}. \tag{36}$$

Since $W_{j,k}\left(\left\{b_i^\star\right\}\right) \le \max\limits_{\{b_i|i\in\mathcal{I}_{j,k}\}} W_{j,k}$, we have $W_{j,k}\left(\left\{b_i^\star\right\}\right) = \max\limits_{\{b_i|i\in\mathcal{I}_{j,k}\}} W_{j,k}$. Therefore, $\left\{b_i^\star | i \in \mathcal{I}_{j,k}\right\}$ is the optimal solution of problem in (20). □

Proof of Theorem 4:

Proof: Since $\Delta W_{i_0,j,k}\left(b^\star_{i_0}\right) < 0$, where $i_0 = \arg\max\limits_i \Delta W_{i,j,k}\left(b_i^\star\right)$, we have $\Delta W_{i,j,k}\left(b_i^\star\right) < 0$ for any $i \in \mathcal{I}_{j,k}$. According to Theorem 1, $\Delta W_{i,j,k}\left(b_i^\star+n\right) < 0$ holds for any $0 \le n \le L$, therefore the objective value of $Q_{j,k}(L_0+1)$ is no more than that of $Q_{j,k}(L_0)$.

Since $\left\{b_i^\star | i \in \mathcal{I}_{j,k}\right\}$ is within the feasible region of problem $Q_{j,k}(L_0+1)$, $\left\{b_i^\star | i \in \mathcal{I}_{j,k}\right\}$ is the optimal solution of problem $Q_{j,k}(L_0+1)$. □

Proof of Theorem 5:

Proof: Since $i_0 = \arg\max\limits_i \Delta W_{i,j,k}\left(b_i^\star\right)$, we have $\Delta W_{i_0,j,k}\left(b^\star_{i_0}\right) \ge \Delta W_{i_2,j,k}\left(b^\star_{i_2}\right)$ for any $i_2 \in \mathcal{I}_{j,k}$. Since $\left\{b_i^\star | i \in \mathcal{I}_{j,k}\right\}$ is the optimal solution of $Q_{j,k}(L_0)$, according to Theorem 2, we have $\Delta W_{i_1,j,k}(b^\star_{i_1}-n) \ge \Delta W_{i_2,j,k}(b^\star_{i_2})$ and $\Delta W_{i_1,j,k}(b^\star_{i_1}-n) \ge 0$ for any $i_1, i_2 \in \mathcal{I}_{j,k}$ and $1 \le n \le L$. Since $\Delta W_{i_0,j,k}\left(b^\star_{i_0}\right) \ge \Delta W_{i_2,j,k}\left(b^\star_{i_2}\right)$ and $\Delta W_{i_1,j,k}(b^\star_{i_1}-n) \ge \Delta W_{i_2,j,k}(b^\star_{i_2})$, we have $\Delta W_{i_1,j,k}(b^+_{i_1}-n) \ge \Delta W_{i_2,j,k}(b^+_{i_2})$. Since $\Delta W_{i_0,j,k}\left(b^\star_{i_0}\right) \ge 0$ and $\Delta W_{i_1,j,k}(b^+_{i_1}-n) \ge 0$, we have $\Delta W_{i_1,j,k}(b^+_{i_1}-n) \ge 0$. Since $\sum\limits_{i\in\mathcal{I}_{j,k}} b_i^\star = L_0$, we have $\sum\limits_{i\in\mathcal{I}_{j,k}} b_i^+ = L_0+1$.

Therefore according to Theorem 3, $\left\{b_i^+ | i \in \mathcal{I}_{j,k}\right\}$ is the optimal solution of problem $Q_{j,k}(L_0+1)$. □

Proof of Theorem 6:

Proof: Assume that there exists $i_0 \in \mathcal{I}_{j,k}$ satisfying $\Delta W_{i_0,j,k}\left(b^\star_{i_0}\right) > 0$. We construct the solution of $\left\{b_i^+ | i \in \mathcal{I}_{j,k}\right\} = \left\{b_i^\star | i \in \mathcal{I}_{j,k}/\left\{i_0\right\}\right\} \cup \left\{b^\star_{i_0}+1\right\}$ satisfying $W_{j,k}\left(\left\{b_i^+\right\}\right) > W_{j,k}\left(\left\{b_i^\star\right\}\right)$, which contradicts with the fact that the optimal solution of problem $Q_{j,k}(L_0)$ is

$\{b_i^\star | i \in \mathcal{I}_{j,k}\}$. Therefore, the assumption is invalid, which means $\Delta W_{i,j,k}(b_i^\star) \leq 0$ holds for any $i \in \mathcal{I}_{j,k}$.

According to Theorem 1, $\Delta W_{i,j,k}(b_i^\star + n) \leq \Delta W_{i,j,k}(b_i^\star) \leq 0$ holds for any $i \in \mathcal{I}_{j,k}$ and $0 \leq n \leq L$, therefore the optimal solution of problem $Q_{j,k}(L_0+1)$ is $\{b_i^\star | i \in \mathcal{I}_{j,k}\}$. □

Proof of Theorem 7:

Proof: Assuming that $\{a_{i,j,k}^\star, b_{i,j,k}^\star | i \in I, j \in J, k \in K\}$ is the optimal solution of problem in (27), we construct another solution as $\{a_{i,j,k}^+ = 1, b_{i,j,k}^+ = a_{i,j,k}^\star \cdot b_{i,j,k}^\star | i \in I, j \in J, k \in K\}$ in the feasible region, and derives

$$W_{i,j,k}^+ = \frac{B}{L} \cdot \left(T - \left(\frac{d_{i,j}}{c} + t_0\right) \cdot \left(1 - a_{i,j,k}^{pre}\right)\right) \cdot a_{i,j,k}^\star \cdot b_{i,j,k}^\star \cdot \log_2\left(1 + \frac{|h_{i,j,k}|^2}{\sigma^2}\right) \cdot \min\left\{\frac{p_{\max}}{\sum_{j=1}^{J}\sum_{k=1}^{K} a_{i,j,k}^\star \cdot b_{i,j,k}^\star + \Delta}, I_{\max}\right\} \quad (37)$$

Since $(T - (\frac{d_{i,j}}{c} + t_0) \cdot (1 - a_{i,j,k}^{pre})) \geq (T - (\frac{d_{i,j}}{c} + t_0) \cdot (a_{i,j,k}^\star - a_{i,j,k}^{pre}))$ and $\sum_{j=1}^{J}\sum_{k=1}^{K} a_{i,j,k}^\star \cdot b_{i,j,k}^\star \leq \sum_{j=1}^{J}\sum_{k=1}^{K} b_{i,j,k}^\star$, we have $W_{i,j,k}^+ \geq W_{i,j,k}^\star$ for any $i \in I, j \in J, k \in K$ and thus $W^+ \geq W^\star$. In addition, since $\{a_{i,j,k}^\star, b_{i,j,k}^\star | i \in I, j \in J, k \in K\}$ is the optimal solution of problem in (27), we have $W^+ \leq W^\star$.

In conclusion, we have $W^+ = W^\star$, which means $\{a_{i,j,k}^+ = 1, b_{i,j,k}^+ = a_{i,j,k}^\star \cdot b_{i,j,k}^\star | i \in I, j \in J, k \in K\}$ is another optimal solution of problem in (27). □

Proof of Theorem 8:

Proof: If $\sum_{i=1}^{I} b_{i,j,k} \leq L$ holds for any $j \in J, k \in K$ and $p_i = \frac{p_{\max}}{b_i}$, the second derivative of W with respect to $b_{i,j,k}$ is always negative, therefore $\Delta W(b_{i,j,k}) < \Delta W(b_{i,j,k} - 1)$. If $\sum_{i=1}^{I} b_{i,j,k} \leq L$ holds for any $j \in J, k \in K$ and $p_i = I_{\max}$, the second derivative of W with respect to $b_{i,j,k}$ is always zero, therefore $\Delta W(b_{i,j,k}) = \Delta W(b_{i,j,k} - 1)$. If $\sum_{i=1}^{I} b_{i,j,k} \leq L$ does not hold for all $j \in J, k \in K$, then $\Delta W(b_{i,j,k}) = \Delta W(b_{i,j,k} - 1) = -\infty$.

In conclusion, $\Delta W(b_{i,j,k}) \leq \Delta W(b_{i,j,k} - 1)$ holds for any $(i, j, k) \in I \times J \times K$. □

REFERENCES

[1] B. Deng, C. Jiang, H. Yao, S. Guo, and S. Zhao, "The next generation heterogeneous satellite communication networks: Integration of resource management and deep reinforcement learning," *IEEE Wireless Commun.*, vol. 27, no. 2, pp. 105–111, Apr. 2020.

[2] X. Zhu, C. Jiang, L. Kuang, Z. Zhao, and S. Guo, "Two-layer game based resource allocation in cloud based integrated terrestrial-satellite networks," *IEEE Trans. Cognit. Commun. Netw.*, vol. 6, no. 2, pp. 509–522, Jun. 2020.

[3] K. An, T. Liang, G. Zheng, X. Yan, Y. Li, and S. Chatzinotas, "Performance limits of cognitive-uplink FSS and terrestrial FS for Ka-band," *IEEE Trans. Aerosp. Electron. Syst.*, vol. 55, no. 5, pp. 2604–2611, Oct. 2019.

[4] G. Zeng, Y. Zhan, and X. Pan, "Failure-tolerant and low-latency telecommand in mega-constellations: The redundant multi-path routing," *IEEE Access*, vol. 9, pp. 34975–34985, 2021.

[5] I. D. Portillo, B. G. Cameron, and E. F. Crawley, "A technical comparison of three low earth orbit satellite constellation systems to provide global broadband," *Acta Astronautica*, vol. 159, pp. 123–135, Jun. 2019.

[6] P. Wan, Y. Zhan, and W. Jiang, "Study on the satellite telemetry data classification based on self-learning," *IEEE Access*, vol. 8, pp. 2656–2669, 2020.

[7] Y. Liu, Y. Chen, Y. Jiao, H. Ma, and T. Wu, "A shared satellite ground station using user-oriented virtualization technology," *IEEE Access*, vol. 8, pp. 63923–63934, 2020.

[8] Y. Zhan, P. Wan, C. Jiang, X. Pan, X. Chen, and S. Guo, "Challenges and solutions for the satellite tracking, telemetry, and command system," *IEEE Wireless Commun.*, vol. 27, no. 6, pp. 12–18, Dec. 2020.

[9] E. Dinc, M. Vondra, and C. Cavdar, "Multi-user beamforming and ground station deployment for 5G direct air-to-ground communication," in *Proc. IEEE Global Commun. Conf. (GLOBECOM)*, Dec. 2017, pp. 1–7.

[10] M. Vondra et al., "Performance study on seamless DA2GC for aircraft passengers toward 5G," *IEEE Commun. Mag.*, vol. 55, no. 11, pp. 194–201, Nov. 2017.

[11] M. Vondra, E. Dinc, and C. Cavdar, "Coordinated resource allocation scheme for 5G direct air-to-ground communication," in *Proc. Eur. Wireless; 24th Eur. Wireless Conf.*, May 2018, pp. 1–7.

[12] Y. Zhu, M. Sheng, J. Li, D. Zhou, and Z. Han, "Modeling and performance analysis for satellite data relay networks using two-dimensional Markov-modulated process," *IEEE Trans. Wireless Commun.*, vol. 19, no. 6, pp. 3894–3907, Jun. 2020.

[13] L. Wang, C. Jiang, L. Kuang, S. Wu, L. Fei, and H. Huang, "Mission scheduling in space network with antenna dynamic setup times," *IEEE Trans. Aerosp. Electron. Syst.*, vol. 55, no. 1, pp. 31–45, Feb. 2019.

[14] L. Wang, C. Jiang, L. Kuang, S. Wu, H. Huang, and Y. Qian, "High-efficient resource allocation in data relay satellite systems with users behavior coordination," *IEEE Trans. Veh. Technol.*, vol. 67, no. 12, pp. 12072–12085, Dec. 2018.

[15] J. Du, C. Jiang, J. Wang, Y. Ren, S. Yu, and Z. Han, "Resource allocation in space multiaccess systems," *IEEE Trans. Aerosp. Electron. Syst.*, vol. 53, no. 2, pp. 598–618, Apr. 2017.

[16] D. Fooladivanda and C. Rosenberg, "Joint resource allocation and user association for heterogeneous wireless cellular networks," *IEEE Trans. Wireless Commun.*, vol. 12, no. 1, pp. 248–257, Jan. 2013.

[17] W. Zhong, Y. Fang, S. Jin, K.-K. Wong, S. Zhong, and Z. Qian, "Joint resource allocation for device-to-device communications underlaying uplink MIMO cellular networks," *IEEE J. Sel. Areas Commun.*, vol. 33, no. 1, pp. 41–54, Jan. 2015.

[18] S. Lohani, R. A. Loodaricheh, E. Hossain, and V. K. Bhargava, "On multiuser resource allocation in relay-based wireless-powered uplink cellular networks," *IEEE Trans. Wireless Commun.*, vol. 15, no. 3, pp. 1851–1865, Mar. 2016.

[19] H. Yu, M. H. Cheung, L. Huang, and J. Huang, "Power-delay tradeoff with predictive scheduling in integrated cellular and Wi-Fi networks," *IEEE J. Sel. Areas Commun.*, vol. 34, no. 4, pp. 735–742, Apr. 2016.

[20] S. Jangsher, H. Zhou, V. O. K. Li, and K. C. Leung, "Joint allocation of resource blocks, power, and energy-harvesting relays in cellular networks," *IEEE J. Sel. Areas Commun.*, vol. 33, no. 3, pp. 482–495, Mar. 2015.

[21] B. Zhao, J. Liu, Z. Wei, and I. You, "A deep reinforcement learning based approach for energy-efficient channel allocation in satellite Internet of Things," *IEEE Access*, vol. 8, pp. 62197–62206, 2020.

[22] A. Ivanov, R. Bychkvo, and E. Tcatcorin, "Spatial resource management in LEO satellite," *IEEE Trans. Veh. Technol.*, vol. 69, no. 12, pp. 15623–15632, Dec. 2020.

[23] A. Destounis and A. D. Panagopoulos, "Dynamic power allocation for broadband multi-beam satellite communication networks," *IEEE Commun. Lett.*, vol. 15, no. 4, pp. 380–382, Apr. 2011.

[24] J. Tang, D. Bian, G. Li, J. Hu, and J. Cheng, "Resource allocation for LEO beam-hopping satellites in a spectrum sharing scenario," *IEEE Access*, vol. 9, pp. 56468–56478, 2021.

[25] C. Han, A. Liu, L. Huo, H. Wang, and X. Liang, "A prediction-based resource matching scheme for rentable LEO satellite communication network," *IEEE Commun. Lett.*, vol. 24, no. 2, pp. 414–417, Feb. 2020.

[26] H. Ma, S. Shen, M. Yu, Z. Yang, M. Fei, and H. Zhou, "Multi-population techniques in nature inspired optimization algorithms: A comprehensive survey," *Swarm Evol. Comput.*, vol. 44, pp. 365–387, Feb. 2019.
[27] H. Shi et al., "Oscillatory particle swarm optimizer," *Appl. Soft Comput.*, vol. 73, pp. 316–327, Dec. 2018.
[28] H. Ma, M. Fei, Z. Jiang, L. Li, H. Zhou, and D. Crookes, "A multipopulation-based multiobjective evolutionary algorithm," *IEEE Trans. Cybern.*, vol. 50, no. 2, pp. 689–702, Feb. 2020.
[29] M. Hong, M. Razaviyayn, Z.-Q. Luo, and J.-S. Pang, "A unified algorithmic framework for block-structured optimization involving big data: With applications in machine learning and signal processing," *IEEE Signal Process. Mag.*, vol. 33, no. 1, pp. 57–77, Jan. 2016.
[30] Z. Lin et al., "Refracting RIS-aided hybrid satellite-terrestrial relay networks: Joint beamforming design and optimization," *IEEE Trans. Aerosp. Electron. Syst.*, vol. 58, no. 4, pp. 3717–3724, Aug. 2022.
[31] Z. Lin, M. Lin, J.-B. Wang, T. de Cola, and J. Wang, "Joint beamforming and power allocation for satellite-terrestrial integrated networks with non-orthogonal multiple access," *IEEE J. Sel. Areas Commun.*, vol. 13, no. 3, pp. 657–670, Jun. 2019.
[32] W. Yu and R. Lui, "Dual methods for nonconvex spectrum optimization of multicarrier systems," *IEEE Trans. Commun.*, vol. 54, no. 7, pp. 1310–1322, Jul. 2006.
[33] H. Tang, J. Wang, L. Song, and J. Song, "Minimizing age of information with power constraints: Multi-user opportunistic scheduling in multi-state time-varying channels," *IEEE J. Sel. Areas Commun.*, vol. 38, no. 5, pp. 854–868, Mar. 2020.
[34] Z. Lin, M. Lin, T. de Cola, J.-B. Wang, W.-P. Zhu, and J. Cheng, "Supporting IoT with rate-splitting multiple access in satellite and aerial-integrated networks," *IEEE Internet Things J.*, vol. 8, no. 14, pp. 11123–11134, Jul. 2021.
[35] M. Albulet, "Spacex non-geostationary satellite system," Federal Commun. Commission, Washington, DC, USA, Tech. Rep. SAT-LOA-20161115-00118, 2016.
[36] A. Paris, I. Del Portillo, B. Cameron, and E. Crawley, "A genetic algorithm for joint power and bandwidth allocation in multibeam satellite systems," in *Proc. IEEE Aerosp. Conf.*, Mar. 2019, pp. 1–15.
[37] K. Ohmaru and Y. Mikuni, "Direct G/T measurement for satellite broadcasting receivers," *IEEE Trans. Broadcast.*, vol. BC-30, no. 2, pp. 38–43, Jun. 1984.
[38] C. Liu, W. Feng, Y. Chen, C.-X. Wang, and N. Ge, "Cell-free satellite-UAV networks for 6G wide-area Internet of Things," *IEEE J. Sel. Areas Commun.*, vol. 39, no. 4, pp. 1116–1131, Apr. 2021.

Guanming Zeng (Graduate Student Member, IEEE) received the B.S. degree in telecommunication engineering from the School of Electronic and Information Technology, Sun Yat-sen University, Guangzhou, China, in 2018. He is currently pursuing the Ph.D. degree in telecommunication engineering with the Department of Electronic Engineering, Tsinghua University, Beijing, China. His research interests include tracking, telemetry and command systems for satellite constellations, and satellite communication networks.

Yafeng Zhan received the B.S.E.E. and Ph.D.E.E. degrees from the Department of Electronic Engineering, Tsinghua University, Beijing, China, in 1999 and 2004, respectively. He is currently an Associate Professor with the Beijing National Research Center for Information Science and Technology, Tsinghua University. His current research interests include satellite TT&C systems, communication signal processing, and deep space communications. He serves as an Editor for *Chinese Space Science and Technology*.

Haoran Xie (Graduate Student Member, IEEE) is currently pursuing the Ph.D. degree in telecommunication engineering with Tsinghua University, Beijing, China. His research interests include application of optimization, machine learning, and statistical theories to communication, fault diagnosis, and resource allocation problems, in particular satellite TT&C systems. He has served as the Chair for IEEE IWCMC 2022 Symposium and IEEE VTC 2022-Fall Symposium.

Chunxiao Jiang (Senior Member, IEEE) received the B.S. degree (Hons.) in information engineering from Beihang University, Beijing, in 2008, and the Ph.D. degree (Hons.) in electronic engineering from Tsinghua University, Beijing, in 2013. He is currently an Associate Professor with the School of Information Science and Technology, Tsinghua University. His research interests include application of game theory, optimization, and statistical theories to communication, networking, and resource allocation problems, in particular space networks and heterogeneous networks. He has also served as a member of the technical program committee as well as the Symposium Chair for a number of international conferences, including IEEE CNS 2020 Publication Chair, IEEE WCSP 2019 Symposium Chair, IEEE ICC 2018 Symposium Co-Chair, IWCMC 2020/2019/2018 Symposium Chair, WiMob 2018 Publicity Chair, ICCC 2018 Workshop Co-Chair, and ICC 2017 Workshop Co-Chair. He has served as an Editor for IEEE INTERNET OF THINGS JOURNAL, *IEEE Network*, and IEEE COMMUNICATIONS LETTERS, and a Guest Editor for *IEEE Communications Magazine*, IEEE TRANSACTIONS ON NETWORK SCIENCE AND ENGINEERING, and IEEE TRANSACTIONS ON COGNITIVE COMMUNICATIONS AND NETWORKING.